Origins of vertical phase separation in P3HT:PCBM mixed films

2014 Jpn. J. Appl. Phys. 53 041601

(http://iopscience.iop.org/1347-4065/53/4/041601)

Japanese Journal of Applied Physics **53**, 041601 (2014) **REGULAR PAPER**
http://dx.doi.org/10.7567/JJAP.53.041601

Origins of vertical phase separation in P3HT:PCBM mixed films

I-Hsiu Liu[1], Yi-Ping Chao[2], Jian-Jhih Fang[2], Wei-Hsuan Tseng[1], Yu-Bing Lan[1], Yu-Jen Chen[3], Kaung-Hsiung Wu[3], and Mei-Hsin Chen[2*]

[1]*Graduate Institute of Photonics and Optoelectronics, National Taiwan University, Taipei 106, Taiwan*
[2]*Department of Opto-Electronic Engineering, National Dong Hwa University, Hualien 974, Taiwan*
[3]*Department of Electrophysics, National Chiao Tung University, Hsinchu 300, Taiwan*
E-mail: meihsinchen@mail.ndhu.edu.tw

Received October 21, 2013; accepted January 13, 2014; published online March 7, 2014

The origins of vertical phase separation and their implication on the device efficiency of poly(3-hexylthiophene):[6,6]-phenyl C61-butyric acid methyl ester (P3HT:PCBM) based solar cells, with both regular and inverted structures, were investigated. We found that the light irradiation and the filtration processes during the device fabrications are two key steps that induce the vertical phase separation in the active layers. Upon light irradiation, the devices with inverted structures exhibit improved power conversion efficiency, whereas the regular devices show degradation. The inverted devices spun cast with filtered P3HT:PCBM solution also present a better improvement as compared to regular devices. X-ray and ultraviolet photoemission spectroscopies indicate that both illumination and filtration enhance the vertical phase separation of the blend film with additional PCBM segregated to the bottom interface.

1. Introduction

Bulk heterojunction (BHJ) polymer solar cells based on a mixture of conjugated polymers and fullerene derivative have the potential advantages of low-cost, lightweight, and flexibility. The interpenetrating network of the donor–acceptor blend offers large interfacial area for efficient charge separation and transport, leading to relatively high power conversion efficiencies.[1–5] However, a nano-scale phase separated morphology has also been observed in several polymer blend systems, resulting in an inhomogeneous distribution of the donor and acceptor components.[6] Concerning poly(3-hexylthiophene):[6,6]-phenyl C61-butyric acid methyl ester (P3HT:PCBM) blends, the vertical phase separation due to the different surface energy of the two components results in a P3HT-rich surface on the air side and PCBM-rich area near the organic/substrate interfaces. This finding suggests that it would be non-ideal for electron collection at the low work function top cathode for the regular-structure devices but would rather make inverted-structure devices, with anode on the top surface, a more promising choice for better energy level alignments.[7,8] Therefore, several studies have been conducted to investigate the parameters influencing the formation of vertical phase separation, such as post annealing, blend composition, viscosity, solvent evaporation rate or substrate surface energy.[9–13] However, there is no report on the change of vertical phase separation due to filtration and illumination, which are two steps that most of the organic solar cell devices would be endured during the fabrication processes and the characterizations. The alteration of vertical phase separation resulting from filtration and illumination might lead to opposite influences on the performance of P3HT:PCBM based devices with conventional or inverted structures.

In this work, we report that filtration of the P3HT:PCBM solution and illuminating on the devices will enhance the vertical phase separation which can greatly improve the performance of the inverted device but degrade the performance of the regular device. The inverted devices, being irradiated with AM1.5G illumination for 30 min, exhibit an evident improvement of power conversion efficiency (PCE) value from 2.7 to 3.4% due to the increase of open-circuit voltage (V_{oc}) and the raise of fill factor. The inverted devices spun cast with filtered P3HT:PCBM solution also present a significant increase in V_{oc} and fill factor. The X-ray photoemission spectroscopy (XPS) measurement demonstrates that PCBM diffuse and segregate more toward the bottom parts of the blend film either with the filtration of the active layer solution or after being irradiated with simulated solar illumination. The results are also supported by atomic force microscopy (AFM) and X-ray diffraction (XRD) measurements. The possible mechanisms which lead to enhanced vertical phase separation are also discussed.

2. Experimental procedure

The organic solar cell devices were fabricated with the following procedures. For the regular structure, a layer of poly(3,4-ethylenedioxythiophene):poly(styrene sulfonate) (PEDOT:PSS) was firstly spin-coated onto the pre-cleaned indium–tin-oxide (ITO) substrate treated with UV–ozone for 15 min. Lithium fluoride (LiF 15 Å) and aluminium (Al 600 Å) were thermally-evaporated as the cathode. For the inverted structure, a thin layer of 0.05 wt % cesium carbonate (Cs_2CO_3) was firstly spin-coated at 6000 rpm onto the pre-cleaned ITO substrate and was annealed at 150 °C for 20 min in a nitrogen-filled glove box. The P3HT:PCBM film with 1 : 1 weight ratio dissolved in 1,2-dichlorobenzene (DCB) was then cast on the Cs_2CO_3 at 900 rpm for 40 s. Some of the devices were spun cast with P3HT:PCBM solution filtered with 0.45 μm syringe filter with poly(vinylidene fluoride) (PVDF) membrane. The samples were then loaded into the vacuum chamber and molybdenum trioxide (MoO_3 15 Å) and silver (Ag 800 Å) were thermally-evaporated as the anode with an active area of 5.5 mm^2.

The samples for XPS and AFM analysis were prepared with the same Cs_2CO_3 and P3HT:PCBM blend solution. To access the active layer and bottom electrode interface, Cs_2CO_3 was dissolved in the water to make the P3HT:PCBM film detach from the substrates. The floating films were then transferred to the gold coated silicon substrates with the buried surface on top. This lifting off method was first proposed by Xu et al.[7] The samples for UPS measurements were prepared in the same way as the samples for making devices before the deposition of MoO_3/Ag and for XPS measurement.

Table I. The performance of solar cell devices with different treatments corresponding to Fig. 1.

		V_{oc} (V)	J_{sc} (mA/cm^2)	FF (%)	PCE (%)	R_{sh} (Ω cm^2)	R_s (Ω cm^2)
Regular	Pristine	0.593	9.91	0.588	3.46	454	8.5
	Irradiated	0.583	9.57	0.589	3.29	440	10.7
	Filtered	0.599	9.59	0.583	3.35	534	9.4
Inverted	Pristine	0.560	9.63	0.508	2.74	475	12.9
	Irradiated	0.582	9.56	0.573	3.35	1587	9.0
	Filtered	0.591	9.20	0.616	3.19	745	10.5

Photoemission measurements were carried out under a base pressure at the order of 10^{-10} Torr. The valence-band ultraviolet photoemission spectra were carried out with He I (21.2 eV) as excitation sources, which is a useful technique for investigate the energy level alignment at the interfaces.[14] The photoelectrons emitted from the sample were captured by a hemispherical analyzer with an overall resolution of 0.05 eV, as determined from the width of the Fermi step measured on a sputter-cleaned gold substrate. The XPS core level spectra were measured via Mg Kα (1253.6 eV) photon lines. The resolution of UPS and XPS are 0.15 and 0.5 eV, respectively.

3. Results and discussion

The current density versus voltage (J–V) curves of organic solar cells under AM1.5G illumination measured in a nitrogen-filled glove box is shown in Fig. 1 and the key parameters are summarized in Table I. The reference devices are spun cast with a non-filtered P3HT:PCBM solution to be compared with the post-treatment of light exposure and pre-treatment of the filtration of P3HT:PCBM solution. For the device with a conventional structure of ITO/PEDOT:PSS/P3HT:PCBM/LiF/Al [Fig. 1(a)], the V_{oc} decreases from 0.59 to 0.58 V which drops the PCE from 3.46 to 3.29% after AM1.5G illumination for 30 min. This result is consistent with the report by Kawano et al.,[15] which suggests that the degradation is caused by carrier accumulation at the vicinity of the electrodes. The accumulated carriers induce reverse bias and drop the V_{oc} gradually under illumination. However, the device with an inverted structure of ITO/Cs_2CO_3/P3HT:PCBM/MoO_3/Ag, shown in Fig. 1(b), presents a performance improvement after AM1.5G illumination for 30 min. The V_{oc} increases from 0.56 to 0.58 V, and the fill factor also improves from 0.51 to 0.57, which raises the PCE from 2.74 to 3.35%. The slight decrease in short circuit current (J_{sc}) (from 9.62 to 9.56 mA/cm^2) with a three-fold increase in shunt resistance indicates the decrease of the leakage current. This result indicates that the illumination has improved the interface morphology between active layer and the electrode of the inverted structure, which can avoid the accumulation of photo-generated carrier and even enhance the PCE. For the inverted structure device spun cast with filtered P3HT:PCBM solution, as shown in Fig. 1(b), a significant increase in V_{oc} (from 0.56 to 0.59 V) and fill factor (from 0.51 to 0.62) are also obtained. The conventional structure device, on the other hand, does not show the obvious improvement in V_{oc} and fill factor with filtered P3HT:PCBM solution [Fig. 1(a)]. This result indicates that illumination on devices and filtration of the active layer are beneficial to the inverted structure rather than conventional one, which is consistent with the advantage of the inverted structure over the conventional structure in terms of the vertical phase separation. Both illumination and filtration of the active solution lead to less leakage current and larger V_{oc} for devices with inverted structures, which can be attributed to improved interface morphology for the inverted devices. The phenomenon of improving efficiency by time for inverted structure is also observed which pushes the device efficiency to 3.77% after three days from fabrication. The improving of V_{oc} and fill factor implies that the growth of efficiency might also be due to the enhancement of vertical phase separation. With more PCBM accumulates near the cathode, a better surface contact is formed to extract photo-generated electrons from PCBM, block the holes leakage from P3HT, and thus increase the V_{oc}.[16]

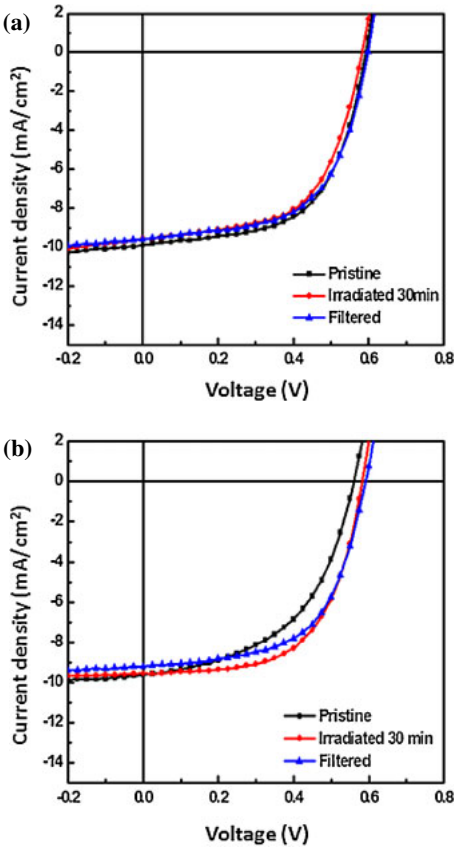

Fig. 1. (Color online) J–V characteristics of the regular and inverted solar cells under AM1.5G illumination measured in a nitrogen-filled glove box. (a) Regular devices with structures of ITO/PEDOT/P3HT:PCBM/LiF/Al. (b) Inverted devices with structures of ITO/Cs_2CO_3/P3HT:PCBM/MoO_3/Ag.

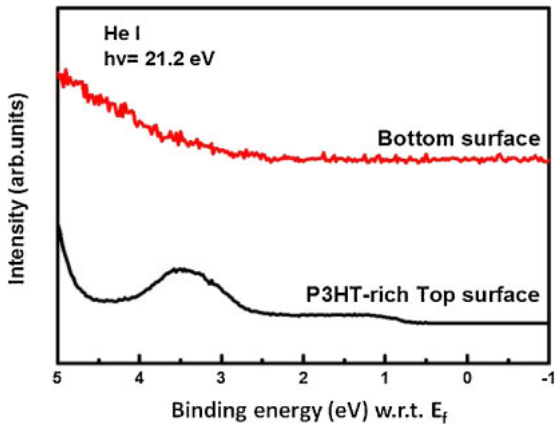

Fig. 2. (Color online) UPS spectra near valence bands of the bottom and top surface of P3HT:PCBM active layers.

To investigate how the vertical phase separation evolved with different process, the valence band spectrum of the top surface and bottom surface of the active layer measured via UPS are shown in Fig. 2. The spectrum of the top surface of the P3HT:PCBM film is almost the same as that of pristine P3HT, with a peak located at 3.5 eV and a tail extending to 0.6 eV below the Fermi level. The spectrum of the bottom surface, on the other hand, does not show the signature peak of P3HT, indicating the lack of P3HT at the bottom surface. The spectrum does not present the PCBM peak as expected since PCBM signals would be more observable with thermal evaporation instead of spin coating, which would result in less order in molecular arrangement. Since the P3HT-rich surface near the cathode is not energetically favorable for electron transport, the electrons might be blocked and accumulate at the interface instead of being collected by the electrode.[15] This result is consistent with our observation of the regular structure device degradation under illumination for 30 min. It is noteworthy that the UPS result of Fig. 2 was obtained from the sample without illumination and filtration to demonstrate the phenomenon of vertical phase separation via comparing the valence band spectrum between top surface and bottom surface of the active layer, instead of comparing the difference between the samples with and without illumination and filtration.

To confirm that the illumination and filtration of the active solution indeed cause different degree of vertical phase separation, the sulfur (S) 2p spectra of the buried interfaces measured via XPS are shown in Fig. 3. The active layer was lifted off and transferred to the Au coated Si substrate with the buried surface on top since the buried surface shows a more distinct variation of surface composition.[7] Since the carbon (C) 1s signal is contributed by both P3HT and PCBM, we compare the S 2p spectra to determine the relative concentration of P3HT and PCBM. In Fig. 3, the peak at around 164 eV is assigned to the thiophene S atoms in P3HT. The peak around 170 eV is related to S atoms in SO_2 which was formed during our fabrication process. Since the XPS spectra in Fig. 3 is from the bottom surface of the active layer fabricated in the structure of ITO/Cs_2CO_3/P3HT:PCBM, the origin of SO_2 comes from the reaction of Cs_2CO_3 with sulfur atoms in P3HT, which represents the bonding between the sulfur atoms connect with oxygen at the interface between the

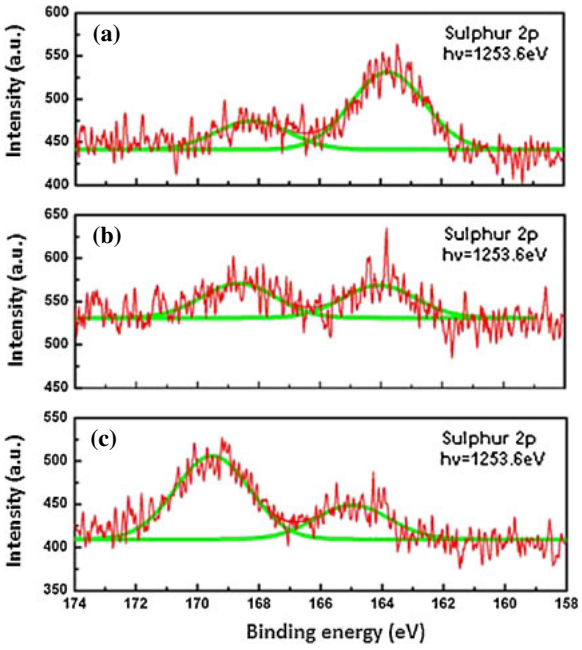

Fig. 3. (Color online) XPS spectra of the S 2p core-level obtained from the bottom surface of P3HT:PCBM films spin coated on Cs_2CO_3 (a) without any treatment, (b) with filtration of the P3HT:PCBM solution, and (c) illuminated after 30 min.

Cs_2CO_3 and the active layer. Moreover, the fabrication process of the Cs_2CO_3 layer for these prepared samples are the same and we do not expect the filtration or illumination would change the bonding of S and O, therefore the signals of SO_2 in all three samples should be at the same level and can be set as the reference. Thus, taking the peak around 170 eV as reference, the intensity of S 2p peak has decreased dramatically after illumination for 30 min [Fig. 3(c)], indicating that the PCBM concentration at Cs_2CO_3/polymer surface is relatively enhanced with light illumination. The irradiation which heats up the device to around 60 °C provides PCBM molecules with kinetic energy to diffuse and enhance the vertical phase separation.[17] Moreover, Cs_2CO_3 layer has been reported to form a strong dipole,[18] which can induce dipole–dipole interaction with PCBM and thus lead to further accumulation of PCBM at the Cs_2CO_3/polymer interface. The increasing amount of PCBM near the anode improves the charge transport at the interface, suppresses the degradation caused by irradiation and even improves the PCE.[19] This mild annealing process by irradiation induces more remarkable vertical phase separation, which enhances the performance of inverted-structure devices but accelerates the degradation of regular-structure devices. Recently, the study of vertical phase separation with pre-annealing temperature above 150 °C has been reported. Our result suggests that the low temperature of the sunlight radiation with the dipole formed by Cs_2CO_3 layer can effectively increase the vertical phase separation of the inverted solar cell.[16] For the film spun cast with filtered P3HT:PCBM solution, it can also be observed that the intensity of S 2p also bears a decrease in S 2p intensity, indicating that the PCBM concentration at Cs_2CO_3/polymer surface is higher. The XPS data proves that the filtration and irradiation will enhance the vertical phase separation which is one of the major reasons for the performance improvement of the inverted-structure device.

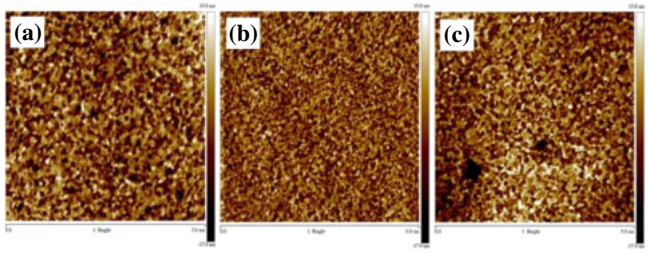

Fig. 4. (Color online) AFM height images of the bottom surface of the P3HT:PCBM film spin coated on Cs_2CO_3 (a) without any treatment, (b) with filtration of the P3HT:PCBM solution, and (c) illuminated after 30 min.

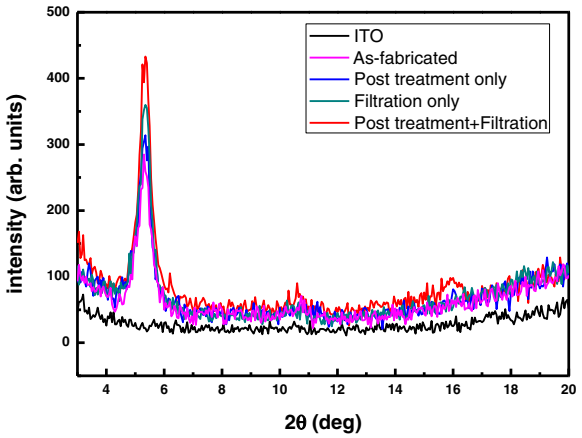

Fig. 5. (Color online) XRD signals from the active layers with different processes.

To understand the morphology evolution with different treatment, AFM was also applied to evaluate the bottom surface of the active layer. Figure 4 shows the height images of the Cs_2CO_3/polymer surface. The as-fabricated film spun cast with solution without filtration is taken as reference with a root mean square (RMS) roughness of 6.27 nm, shown in Fig. 4(a). In comparison, Fig. 4(b) presents that the film spun cast with filtered P3HT:PCBM solution has relatively small grain size and a smoother surface with a RMS roughness of 4.93 nm. This result shows that the filtration process has altered the nanostructure of the organic layer. The filtration process might have weed out the impurities and some of the larger P3HT polymers which are less soluble in DCB and therefore results in a more suitable condition for P3HT and PCBM crystallization. As P3HT and PCBM are mixed more homogeneously with smaller size in DCB, the vertical phase separation is enhanced during the solvent evaporation process since both P3HT and PCBM can move more freely and accumulate at the interface to achieve the minimum overall energy,[6,20] which is coincident with XPS result. For the film irradiated for 30 min, the AFM result, which is shown in Fig. 4(c), does not show a distinct difference with the one before irradiated. The temperature of the irradiation is not high enough to reach the glass-transition temperature of P3HT to re-crystalize but can provide PCBM with enough energy to diffuse and accumulate more at the bottom interface.

In order to understand the crystallization of P3HT molecules under different processes, the XRD measurement has also been carried out on the active layers, including the as-fabricated samples, samples with post treatment or filtration, and samples with both post treatment and filtration. As shown in Fig. 5, the XRD data reveals that the intensity of the P3HT (100) peaks from the sample with both post treatment and filtration is the highest, indicating that it is more favorable for the polymer to crystallize and form phase separation after both post treatment and filtration.

4. Conclusions

In conclusion, the influences of filtration of the active layer solution and the illumination on both regular and inverted devices are studied. A detailed XPS analysis reveals that both treatments lead to more remarkable vertical phase separation of the donor and acceptor components, with less P3HT but more PCBM molecules segregate at the bottom interface. This observation is consistent with the opposite trend of device performance demonstrates by inverted devices and regular devices. Compared to the degradation of regular devices, the inverted devices exhibit an evident improvement in PCE value from 2.7 to 3.3% after 30 min of illumination. The device with inverted structure benefits from the illumination and filtration in terms of vertical phase separation, resulting in improvement in device performance.

Acknowledgement

This research was financially supported by National Science Council, the Republic of China under Contract No. NSC 101-2112-M-259-004-MY2.

1) S. R. Forrest, Nature **428**, 911 (2004).
2) H. Hoppe and N. S. Sariciftci, J. Mater. Chem. **16**, 45 (2006).
3) S. K. M. Jönsson, E. Carlegrim, F. Zhang, W. R. Salaneck, and M. Fahlman, Jpn. J. Appl. Phys. **44**, 3695 (2005).
4) J. You, T. Arakawa, T. Munaoka, T. Akiyama, Y. Takahashi, and S. Yamada, Jpn. J. Appl. Phys. **50**, 04DK22 (2011).
5) M. Campoy-Quiles, T. Ferenczi, T. Agostinelli, P. G. Etchegoin, Y. Kim, T. D. Anthopoulos, P. N. Stavrinou, D. D. C. Bradley, and J. Nelson, Nat. Mater. **7**, 158 (2008).
6) Y. Vaynzof, D. Kabra, L. Zhao, L. L. Chua, U. Steiner, and R. H. Friend, ACS Nano **5**, 329 (2011).
7) Z. Xu, L.-M. Chen, G. Yang, C.-H. Huang, J. Hou, Y. Wu, G. Li, C.-S. Hsu, and Y. Yang, Adv. Funct. Mater. **19**, 1227 (2009).
8) L.-M. Chen, Z. Hong, G. Li, and Y. Yang, Adv. Mater. **21**, 1434 (2009).
9) P. G. Karagiannidis, D. Georgiou, C. Pitsalidis, A. Laskarakis, and S. Logothetidis, Mater. Chem. Phys. **129**, 1207 (2011).
10) C. Waldauf, M. Morana, P. Denk, P. Schilinsky, K. Coakley, S. A. Choulis, and C. J. Brabec, Appl. Phys. Lett. **89**, 233517 (2006).
11) M. N. Yusli, T. W. Yun, and K. Sulaiman, Mater. Lett. **63**, 2691 (2009).
12) Y. S. Kim, Y. Lee, J. K. Kim, E.-O. Seo, E.-W. Lee, W. Lee, S.-H. Han, and S.-H. Lee, Curr. Appl. Phys. **10**, 985 (2010).
13) W.-H. Baek, T.-S. Yoon, H. H. Lee, and Y.-S. Kim, Org. Electron. **11**, 933 (2010).
14) N. Koch, A. Elschner, R. L. Johnson, and J. P. Rabe, Appl. Surf. Sci. **244**, 593 (2005).
15) K. Kawano and C. Adachi, Adv. Funct. Mater. **19**, 3934 (2009).
16) N. Li, B. E. Lassiter, R. R. Lunt, G. Wei, and S. R. Forrest, Appl. Phys. Lett. **94**, 023307 (2009).
17) O. Yoshikawa, T. Sonobe, T. Sagawa, and S. Yoshikawa, Appl. Phys. Lett. **94**, 083301 (2009).
18) J. Huang, G. Li, and Y. Yang, Adv. Mater. **20**, 415 (2008).
19) A. Orimo, K. Masuda, S. Honda, H. Benten, S. Ito, H. Ohkita, and H. Tsuji, Appl. Phys. Lett. **96**, 043305 (2010).
20) S. Y. Heriot and R. A. L. Jones, Nat. Mater. **4**, 782 (2005).